Global Properties and Local Structure of the Weather Attractor over Western Europe

CHRISTIAN L. KEPPENNE

Institut des Sciences Naturelles Appliquées, Louvain-la-Neuve, Belgium

C. NICOLIS

Institut d'Aéronomie Spatiale de Belgique, Bruxelles, Belgium

(Manuscript received 10 February 1988, in final form 16 January 1989)

ABSTRACT

An analysis of the West European climate over short time scales is performed by means of time series of the 500 mb geopotential height at nine different meteorological stations. The characterization of the dynamics is based on the computation of the dimensions of manifolds on which the systems evolve. For this purpose several embedding techniques are used and compared. All methods give similar results, namely, that the data in different stations seem to derive from a single deterministic dynamical system spanning a relatively low-dimensional manifold embedded in a low dimensional phase space. The estimation of the most significant Lyapounov exponents of the global system gives evidence that the nature of the dynamics is chaotic. The average *e*-folding time scale of the "growth of errors" associated with divergence of nearby initial conditions is found to be a few weeks. A more involved analysis reveals that the Western European weather attractor is highly nonuniform, expressing the fact that the stability properties of the trajectories depend on their position on the manifold. It is found that the predictability time in the regions of the attractor which correspond to low geopotential heights is slightly above one month decreasing to about two weeks for high geopotential values. The connection between these estimates and the error growth time determined from numerical models of weather prediction is discussed.

1. Introduction

Since weather and climate apparently have a very complicated distribution in time and space, the usual approach for improving their predictability is to introduce increasingly more variables and equations in the very complex numerical models used to simulate atmospheric dynamics. A typical example is found in weather forecasting where the complexity of the models tends to grow commensurately with the capacity of supercomputers. Unfortunately, despite impressive progress in short term forecasting this has not resulted in commensurate improvements of the reliability of forecasts on a time scale exceeding a few days.

Recent developments of the theory of dynamical systems have provided new techniques by which important qualitative information can be extracted from experimental time series. This suggests that it should now be possible to learn more about the underlying dynamics of weather and climate and to find to what extent they are predictable, independent of any modeling. The steps of such an analysis can be summarized as follows.

First, one has to gain evidence that the system shows the typical signs of a dissipative deterministic dynamics, that is to say, that it evolves on an attracting manifold of zero volume in some finite-dimensional phase space. Having ascertained this, one may proceed with the determination of some of its qualitative properties, such as the dimension of the manifold itself and of phase space in which it is embedded, and the *Lyapounov exponents*. Basically, the dimension of the attracting manifold measures to what extent its dynamics fills the embedding phase space, whereas the dimension of phase space provides an estimate of the smallest number of ordinary differential equations sufficient to describe the time evolution of the dynamical system. The Lyapounov exponents are related to the average rates of divergence of nearby trajectories in phase space and measure, therefore, how unpredictable the system's evolution is.

Although the new developments and concepts mentioned above have found most of their applications in theoretical studies of iterative maps and abstract model systems, they have also provided important insights in the analysis of results of laboratory experiments. Recently, Nicolis and Nicolis (1984, 1985) applied these ideas in the context of Geophysics by analyzing time series of $\delta^{18}O$ isotope record of deep sea cores. They concluded in the existence of a low- (about three) dimensional attractor and a predictability time of about 30 kiloyears (kyr). Subsequently, Fraedrich (1986, 1987), Essex et al. (1987), Hense (1987) and Tsonis

Corresponding author address: Dr. C. Nicolis, Institut d'A'eronomie Spatiale de Belgique, 3 Avenue Circulaire, B 1180 Brussels, Belgium.

and Elsner (1988) analyzed time series of medium and short time scales and have likewise concluded about the existence of low-dimensional attractors.

Our goal in the present work is to carry out a dynamical systems analysis of atmospheric variability over the *entire* West European space. For this purpose we analyze geopotential time series using data from a number of stations.

Since we only have a limited number of data points in our disposal, we take special care to control at each stage of the analysis the applicability of the various algorithms (Grassberger 1986; Nicolis and Nicolis 1987). For instance, we apply several phase space reconstruction techniques to compute the dimensions of attracting manifolds and of embedding spaces; we also test each of the techniques used on the time series generated by some known mathematical models, limited to a number of points comparable to our data points. We have obtained very similar results with all methods, although we found that the one based on the reconstruction of a phase space spanned by empirical orthogonal functions diminished the error margins of our dimension estimates. In addition, we have found it possible to estimate with relative accuracy the largest Lyapounov exponents for the West European system as a whole. These results, and their corrolaries emanating from the local study of the rates of divergence of nearby trajectories on the attractor, are entirely new in the context of atmospheric sciences. They have allowed us to extract additional information about the topology of the weather attractor, to estimate a characteristic predictability time scale for the dynamics of our system and to confront it with the estimate of error growth time deduced from numerical models of weather prediction.

The work is organized as follows. In section 2 we present the data, comment on the adequacy of the sampling time and of the total length of the series, and carry out traditional spectral analysis. The results show striking similarities between the different time series. In section 3 we set up an appropriate phase space within which the dynamics can be followed. In section 4 we produce evidence that the phase space trajectories evolve on a low-dimensional manifold, the attractor. The dimensionality of the latter is evaluated and found to be similar for all locations. This corroborates the idea that individual time series are part of a single dynamical system. In section 5 it is shown that the motion on the attractor displays sensitivity to initial conditions. The Lyapounov exponents describing this sensitivity are evaluated and found to be state-dependent, indicating that the predictability time should depend on the prevailing weather pattern. The implications of the results are briefly discussed in section 6.

2. The data and their spectral properties

We were supplied with time series of the daily 500 mb geopotential record at nine different European stations over a period of 24 years beginning 1 January 1961. The precision was the same for all series, the geopotential height being rounded to the nearest decameter. Two stations (Marseille and Rome), are situated in the Mediterranean sea, two (Lisbon and Bordeaux) are on the Atlantic coast, one (Stockholm) is in Scandinavia, another (Reykjavik) in Iceland, and the others (De Bilt, London and Paris) surround the Channel and the North Sea area. Figure 1 depicts the time dependence of the 500 mb geopotential height for the Marseille station.

Before we proceed to the technical aspects of our work, we comment on a number of qualitative issues concerning the very objective followed in the present paper, in connection with the data we have at our disposal. Two particularly important points need to be considered: the inherent discretization of the data with a sampling time of one day; and the total number of data points (about 9000 for each station) or alternatively, the number of annual cycles (24 in our case) retained.

As stated in the Introduction, our objective is "to carry out a dynamical systems analysis of atmospheric variability over the entire West European space." Such a goal seems at first sight far too ambitious; some comments aiming to sharpen it somewhat are therefore in order.

Atmospheric and climate dynamics involve a bewildering variety of phenomena in a wide range of time and space scales (Hasselmann 1976; Lorenz 1987). In principle, all these phenomena are included in the fundamental equations of conservation of macroscopic physics, supplemented with adequate thermodynamic relations and specific laws pertaining to the light-matter interaction. It is not our aim here to capture this entire dynamics in all its details. On the one side such processes as the formation of a droplet of water or of a cumulus cloud, and the fine details of fully developed turbulence are below the one-day resolution of our data; and on the other side the effect of such phenomena as the dynamics of ice sheets or of the sun's 22-

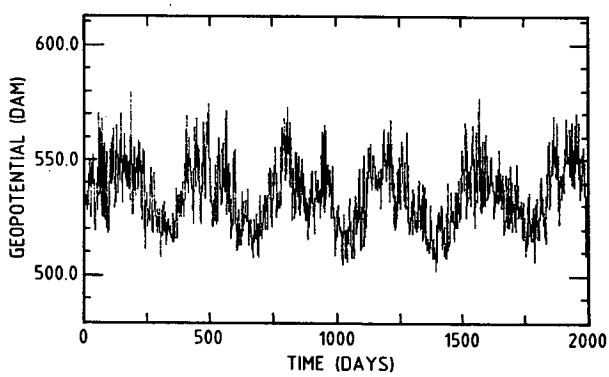

FIG. 1. Time evolution of the 500 mb geopotential height at Marseille.

year cycle are beyond the 24-year range spanned by our data. What we want to see instead, is whether there exists an autonomous deterministic dynamics accounting for the main features of the record in the intermediate range between a day and a few decades, which is largely independent of the phenomena occurring on both much shorter and much longer scales.

The possibility of a drastic reduction of the description of a complex system envisioned by the above argument is by no means new. In physics for instance, it is at the basis of the validity of such well-accepted laws as macroscopic hydrodynamics and chemical kinetics. As well known the passage between the dynamics at the molecular level and these macroscopic laws rests on the fact (Belescu 1975) that the quantities obeying to macroscopic laws are averages of microscopic quantities; the averaging being taken over a statistical ensemble or over a time interval much longer than the characteristic times of the dynamics of a simple molecule, such as the duration of an intermolecular collision (10^{-13} sec). Typical hydrodynamic or chemical "sampling" times are therefore of the order of a millisecond. It has been pointed out (Caputo et al., 1986; Atmanspacher et al. 1988) that a valuable criterion for choosing this time is to have about ten data points into a correlation period of the process, the latter being determined by an autocorrelation function analysis. Too few data points per correlation time yield a spurious, uncorrelated (stochastic) process. As for the upper limit of resolution a practical indication is to avoid very small differences in successive signal amplitudes which could possibly be blurred by the counting statistics. Regarding the total length of the time series, noisy datasets of 500 points or so have been shown to be sufficient for the approximate estimate of the correlation dimension of chaotic attractors, if the latter is not very large (Abraham et al. 1986). For more detailed information such as the spectrum of the Lyapounov exponents or higher order dimensions more data are needed.

Let us now have a critical look at our dataset in the light of the above remarks. We first comment on the resolution of one day. It has been pointed out (Ghil and Childress 1987; Ghil 1987) that the typical life cycle of a traveling cyclone in midlatitudes is in the 5–7 day range and that the characteristic relaxation time of vorticity at the equivalent barotropic level in midtroposphere is of the order of 10 days. Clearly the sampling time of the 500 mb geopotential, a quantity directly related to the above processes, should be significantly less. This brings us to the one-day scale (the highest resolution of the geopotential record available is one-half day). For an additional confirmation of the adequacy of this sampling we must turn to the correlation function and spectral analysis of our data. This will be reported in detail later on in this section. Suffice it to state here that a reasonable estimate of the correlation period appears to be 9 to 15 days (depending on the station considered), in view of which the one-day sampling time appears again to be quite reasonable.

Turning next to the total length of the time series, it should first be mentioned that no daily record of geopotential spanning an appreciably longer period of time is currently available. If, as pointed out earlier, ~500 points are sufficient to estimate low correlation dimensions (Abraham et al. 1986) it is not unreasonable to expect that with 9000 data points that we have at our disposal we can go much further in the analysis of the subsequent sections.

Despite the above rather reassuring remarks, in order to control as much as possible any spurious effects that might still subsist, we will constantly compare all results of data analysis with those of mathematical models whose dynamics has been extensively studied. Those "reference" systems are (a) the Lorenz and Rössler systems (Lorenz 1963; Rössler 1979), known to exhibit chaotic dynamics, (b) simple periodic signals, and (c) a numerical pseudorandom number generator. In each case the time series extracted from these models is chosen to have the same number of points, the same accuracy and the same mean number of orbital periods on the attractor as the geopotential signal (for which the mean orbital period corresponds to the annual cycle).

For subsequent reference we give below the evolution equations of the Rössler and Lorenz models and the corresponding parameter values for which both models give rise to a chaotic attractor:

Rössler model

$$\begin{aligned} \dot{x} &= -(y + z) \\ \dot{y} &= x + ay \\ \dot{z} &= bx + z(x - c) \end{aligned} \tag{1}$$

with $a = 0.15$, $b = 0.20$, $c = 10.0$.

Lorenz model

$$\begin{aligned} \dot{x} &= \sigma(y - x) \\ \dot{y} &= x(r - z) - y \\ \dot{z} &= xy - bz \end{aligned} \tag{2}$$

with $\sigma = 16.0$, $r = 45.92$, $b = 4.0$.

Let us return to the geopotential signal. In order to get some feeling about some general features of the signals we shall perform in this section traditional spectral and correlation function analysis, postponing a more dynamical approach until section 3.

a. Power spectra

The most familiar method of data analysis is the spectral method. It is well known that spectral estimates obtained by the standard FFT algorithm fluctuate with an exponential distribution about the theoretical sample spectrum (square of the modulus of the Fourier

transform). Therefore, it is more difficult to observe frequency peaks in the corresponding spectra than in those obtained using a smoothing artifact because peaks are masked by uncontrolled large amplitude oscillations.

The computation of unsmoothed spectra involves consideration of all autocorrelation coefficients (Wax 1954)

$$\tilde{\psi}_k = \sum_{j=1}^{N-k} X_j X_{j+k}, \quad k = 1, \cdots, N \tag{3}$$

$\{X_i\}$ being the time series and N the total length. Smoothed spectra are deduced from the set of the first m covariances whereby the width m of the window satisfies $m < N$. As the bandwidth of the resulting spectrum is proportional to $1/m$, the spectral estimates are reliable only over a frequency separation larger than the bandwidth.

We have computed the smoothed spectra using the Tukey window and a width of 6 mon. In this procedure the correlation coefficients $\tilde{\psi}_k$ are weighted by

$$w_k = \frac{1}{2}\left[1 + \cos\left(\pi \frac{k}{m}\right)\right]. \tag{4}$$

As expected, the spectra of the nine signals display a very clear peak corresponding to the annual cycle. All are predominently red and tend to become white beyond a cutoff frequency of about 0.4 cycles per day (cpd). The spatial average of all signals has a power spectrum which is qualitatively similar (same peak and general shape) to that of a single time series (compare Figs. 2a and 2b).

Notice that from the above analysis alone one cannot have clear-cut information on the underlying dynamics. Namely, it is impossible to decide whether one deals with noisy periodic—or quasi-periodic—signals or whether the dynamics are chaotic, experiencing sensitivity to initial conditions (Brock and Chamberlain 1984). For instance, truncated to the same number of bits, the variable x of Rössler's model [Eq. (1)] has a continuous spectrum similar to that displayed in Figs. 2. In addition, it is well known that second or higher order autoregressive models can also produce similar behavior.

In fact, a simple sinusoid of one-year period will give the appearance of a continuous spectrum centered on a well-defined peak merely because of discretization. Naturally, on increasing the sampling precision this latter spectrum will tend to a line spectrum, whereas the spectrum will remain continuous for deterministic chaos or random noise. Nevertheless, these remarks show how cautious one has to be in treating data in which the sampling precision has been specified once for all. Clearly, in order to extract the dynamics from such data a confrontation of results from different methods of analysis becomes necessary.

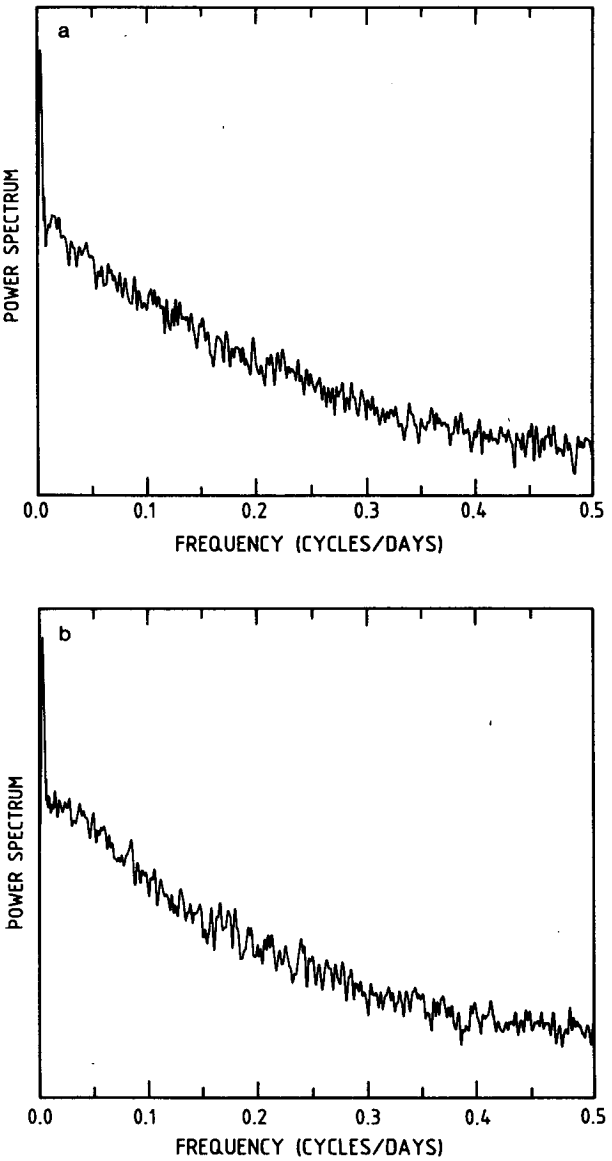

FIG. 2. (a) Smoothed power spectrum of the daily 500 mb geopotential at Marseille (b) smoothed spectrum obtained from spatial averaging of the signal at nine stations.

b. *Time correlation functions*

The normalized time correlation ψ of a discrete signal X, constituted of n samples X_i equally spaced in time, is defined as

$$\psi_k = \frac{\frac{1}{N-m}\sum_{i=1}^{N-m} X_i X_{i+m}}{\frac{1}{N}\sum_{i=1}^{N} X_i^2}. \tag{5}$$

It has the following properties. Except for a proportionality factor, it is the inverse Fourier transform of

the sample spectrum of the signal itself. It oscillates indefinitely for a periodic or quasi-periodic signal whereas for a wide class of Markov processes and of deterministic chaotic attractors it goes through zero at some finite time or tends asymptotically to zero as $t \to \infty$. On the other hand, for Gaussian white noise the zero is immediately attained. We compared the time correlation function of our datasets with those obtained from the discretization of Rössler chaos, a sum of two sines and a pseudorandom signal.

The correlation functions of our signals tend to zero in a finite time and the same tendency is exhibited by both the rounded off Rössler chaos [Eq. (1)] and a truncated sinusoid though, as mentioned above, in the latter case the properties depend critically on the resolution adopted. In Figs. 3a and 3b the time correlation function corresponding to the station of Marseille is compared to the one obtained by the spatial average of all signals. Note that a qualitative difference of ψ between the individual signals is that the more southerly a station is situated, the faster the amplitude of the oscillations of the correlation function decrease.

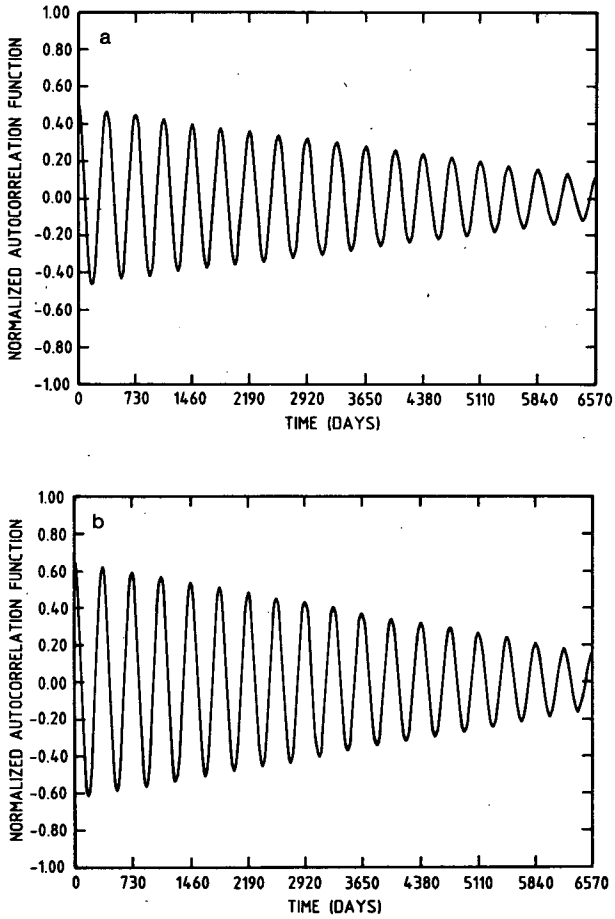

FIG. 3. Correlation function of the geopotential signal over large time scales: (a) Marseille, (b) spatial average of nine signals.

This suggests that the periodic part of the dynamics is less pronounced for the southern stations.

As pointed out earlier in this section the correlation time—the time that must elapse between two samplings to obtain statistical independence—is an important characteristic of our system. In a multivariate process likely to involve a variety of characteristic time scales, such as the process studied in the present work, it is not easy to estimate such a time unambiguously. Nevertheless, one can argue that the time at which the first inflexion point is observed in the graph of the autocorrelation function versus time provides a valuable indication. Indeed, using the standard properties of correlation functions one easily sees that (Balescu 1975):

$$\ddot{\psi}(\tau) = \langle X(0)\ddot{X}(\tau)\rangle = -\langle \dot{X}(0)\dot{X}(\tau)\rangle. \quad (6)$$

It follows that $\ddot{\psi}(\tau)$ vanishes [i.e., $\psi(\tau)$ has an inflexion point] when the rate of change of X becomes uncorrelated from its initial value. Intuitively, this conclusion is appealing since the rate of change of a variable is a more significant indication of the dynamics than the variable itself.

Inspection of the short time behavior of the autocorrelation function of our signal shows that the first zero of $\ddot{\psi}$ occurs in 9 to 15 days, depending on the station. This scale turns out to be in accordance with the characteristic time scales likely to be related to our variable alluded to in the beginning of this section. We can therefore infer from these arguments that a reasonable value of the correlation time is in this same range.

In summary, although it is premature to draw general conclusions about the nature of the underlying dynamics we are, nevertheless, able to make the following two statements:

- Neither of the series displays the signs of a completely random behavior, since none of the correlation functions falls to zero within a very short time. However, it is not clear as yet whether the dynamics is periodic, quasi periodic, first or higher order Markovian, or exhibits sensitivity to initial conditions.
- There seems to be a single overall dynamics for all stations, since results corresponding to individual signals are similar.

3. Phase space reconstruction: Time delays and principal component analysis

Our next objective is to go beyond the limited view afforded by spectral analysis and reconstruct some of the salient features of the dynamics. To achieve this we need to embed the evolution of our system in *phase space,* the space spanned by the full set of its relevant variables. Ordinarily, in mathematical modeling or in laboratory experiments the state variables are known

in advance since one deals with a well-defined set of evolution laws. However, in a natural system this full information is lacking: for instance, in the system of interest in the present paper all we have at our disposal is the geopotential time series at a given location,

$$X_1(t_i): X_0(t_1), X_0(t_2), \ldots, X_0(t_N) \qquad (7)$$

where t_1 is the initial time (1 January 1961) and $\Delta = t_2 - t_1 = \cdots = t_N - t_{N-1}$ is the sampling time (1 day).

It has been shown by Takens (1981) that from a single time series one can actually reconstruct properly a phase space, by considering (7) as well as the hierarchy of lagged variables

$$\begin{aligned} X_2(t_i)&: X_0(t_1 + \tau), X_0(t_2 + \tau), \ldots, X_0(t_N + \tau) \\ &\vdots \\ X_n(t_i)&: X_0[t_1 + (n-1)\tau], X_0[t_2 + (n-1)\tau], \ldots, \\ &\quad X_0[t_N + (n-1)\tau]. \end{aligned} \qquad (8)$$

Indeed, if τ is properly chosen the variables $X_1, \ldots, X_n$ will typically be independent, and this is all one needs to define a phase space.

Owing to the limitations related to sampling, τ will necessarily be an integer multiple of Δ, $\tau = m\Delta$. If the last measurement at our disposal is $X_0(t_N)$, then clearly the variable X_n has at most $N_T = N - (n-1)m$ data points. In what follows, therefore, we shall limit all other variables to the same number of data. At this stage of development we have no means to specify the value of n. What is achieved is merely the possibility to plot, for increasingly large n, the phase space trajectory of the system and draw some preliminary conclusions about its complexity. This may also be useful for determining a range of values of the lag τ allowing an optimal visualization of the dynamics.

Figure 4 gives a three-dimensional view of the trajectory for the Marseille time series (Fig. 1). We see that the portrait fills the entire space suggesting that the system lives in a higher than three-dimensional phase space.

Another method of reconstruction of phase space is closely connected to a familiar question in geosciences, namely how to determine the directions of *maximum variability*. This is usually achieved by the so-called principal component, or empirical orthogonal function (EOF), analysis (for instance, see North et al. 1982). More precisely, EOFs are just the eigenvectors of the covariance matrix, i.e., of the matrix of quadratic averages (in the present context "averaging" is a mean over all data points). They therefore describe variables that are statistically independent up to third or higher order correlations. Clearly the EOFs corresponding to the largest eigenvalues will correspond to the directions of maximum variability.

If the variables are reconstituted from the time series of a single variable as in (7), the covariance matrix will be of the form

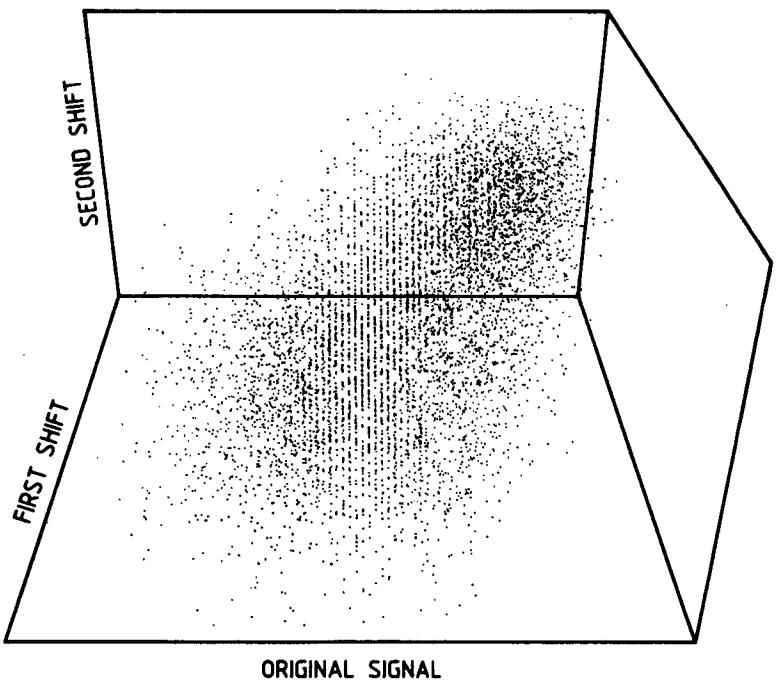

FIG. 4. Three-dimensional projection of the entire trajectory for Marseille obtained by the method of time delays, with a shift $\tau = 10$ days.

$$\Phi_{ij} = \frac{1}{N_T} \sum_{k=1}^{N_T} X_0(t_K + i\tau) X_0(t_k + j\tau)$$

$$i, j = 0, \cdots, n-1. \quad (9)$$

In the following we will denote the eigenvalues of the covariance matrix as $\lambda_1 > \lambda_2 > \cdots > \lambda_n$ and the corresponding eigenvectors by $c_1, \ldots, c_n$. The space spanned by these latter vectors will be referred to as singular space (Broomhead and King 1986). Embedding our dataset into this space amounts therefore to switching from the state vector $\mathbf{X} = \{X_1, \cdots, X_n\}$ to a state vector

$$\mathbf{Y} = \mathbf{Xc} \quad (10)$$

where $\mathbf{c}$ is an $n \times n$ matrix whose columns are the eigenvectors $\mathbf{c}_i$.

In addition to providing a natural way to visualize the dynamics, EOFs may also be of interest in the following respect. It may happen (as it will be the case in the problem under consideration) that among the n eigenvalues λ_i there exists a limited number of distinct ones whose magnitude is appreciable, whereas the others are all close to zero. If so, this would be a strong indication that the dynamics contains a "deterministic" part in the subspace of the distinct eigenmodes, whereas the other modes will play the role of "noise." It is, however, not possible to distinguish on this sole basis between noise of random origin or a noise related to an underlying chaotic dynamics. For instance, North et al. (1982) show that when the difference between two nearby eigenvalues of the covariance matrix is comparable to the sampling error of the corresponding true EOFs, the sampled EOFs can form a degenerate multiplet. In such a case, the components of the multiplet's members will be some linear combination of those of the true EOFs associated to the geopotential field. This is what is referred to as mixing. The same authors also propose the following simple rule of thumb to determine whether effective degeneracy is susceptible to occur. If the difference $\lambda_j - \lambda_{j+1}$ is about or less than $\lambda_j(2/N_T)^{1/2}$, the components of c_j and c_{j+1} are likely to mix. Thus, if in this case we truncate the dynamics by retaining a j-dimensional projection of the trajectory onto the subspace spanned by the first j EOFs, we will lose some information over the time scale associated to λ_j and retain information over the time scale corresponding to λ_{j+1}. However, we may still truncate to the first $j + 1$ EOFs if none of them mixes with some EOF of higher order. In short, it is generally impossible to estimate the dimension of the attractor on the sole basis of singular space analysis.

Another problem arising in the use of EOFs for the reconstruction of phase space pertains to the choice of the width of the window ($\tau \times n$). If the latter is excessively small it can result in an underestimation of the number of singular values above the noise floor and a set of EOFs containing information solely on the dynamics over the shorter time scales. After several trials, we found that the best choice of the width was about 6 months for an 18×18 covariance matrix, corresponding to a lag $\tau \sim 10$ days. This is consistent with the requirement (for instance, see Mayer-Kress 1986) that the optimal range of lag τ, both for visualization of the attractor and for the applicability of the various algorithms, is given by the correlation time of the signal.

In Fig. 5 we represent the first six eigenvalues and the corresponding EOFs of an 18×18 covariance matrix for the 500 mb height at one station. We can see that mixing appears after the first three vectors. The signals corresponding to the other stations, the spatial average of all nine time series as well as the signal obtained by concatenating the individual series give comparable results. For comparison we show in Fig. 6 the first six eigenvalues and eigenvectors of a pseudorandom signal. The difference with Fig. 5 is striking: mixing is immediate as the eigenvalues are all of comparable size. This indicates that all space directions spanned by the EOFs are explored to the same extent by the dynamics.

The preliminary analysis performed in the preceding section suggests that all nine datasets describe the same kind of dynamics, and in the next section we shall produce further evidence corroborating this idea. Assuming then that this view is legitimate, we may use a third alternative for the phase space reconstruction of our system based on the "multichannel" variables corresponding to the different spatial locations, instead of the time lag variables of a single location. In the present case the number of different space locations is limited to nine. Since we do not know offhand the phase space dimensionality we will use a "mixed" representation in which each spatial channel is enlarged to a number of lagged variables obtained from the original time series. As it will turn out these approaches yield similar results.

4. Dimensions of weather attractor and of embedding phase space

a. Methods

Having identified the variables that will span the phase space and the way they can be obtained from the original time series, we shall now characterize the nature of the trajectories of our dynamical system in this space. To this end we shall proceed as follows:

(i) Choose increasingly large values of embedding dimension n, and for each n plot the values of $\mathbf{X} = (X_1, \cdots, X_n)$ for the N_T data points [cf. Eq. (8)].

(ii) For each n, determine the dimension, ν, of the above plotted dataset.

(iii) Study the dependence of ν for increasing n. If

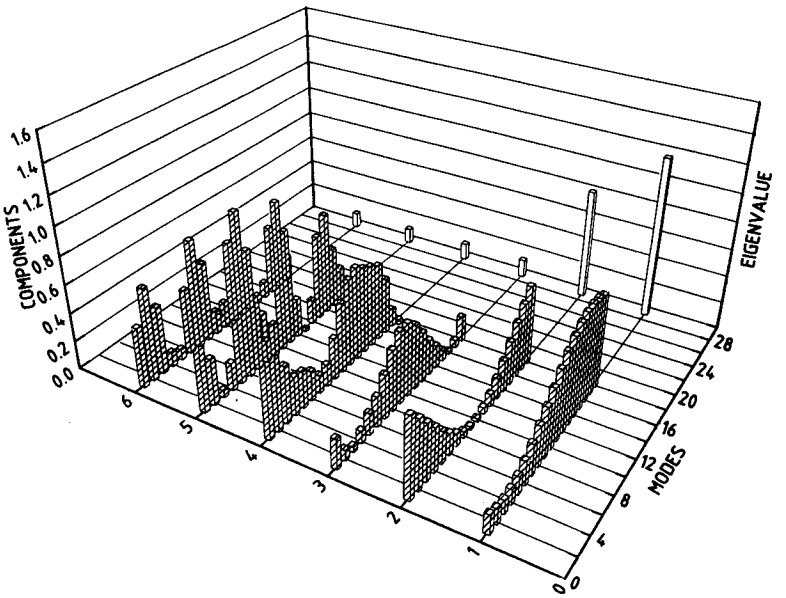

FIG. 5. Eigenvalues (white blocks) and eigenvectors (hatched blocks) of an 18×18 covariance matrix for the signal at Marseille. The vertical axis has been shifted upwards by 0.5.

this dependence saturates to some value ν_s beyond a certain reasonably small n_s, we will conclude that our system is a deterministic dynamical system possessing a dimension ν_s. As for n_s, it will represent the minimum number of variables needed to describe the dynamics.

In dynamical systems theory one defines a whole hierarchy of dimensions, but for our purposes it will suffice to focus on the *correlation dimension* ν (for instance, see Mayer-Kress 1986). The idea is to choose at random a point $\mathbf{X}_i$ of our dataset in phase space and count the number of other data points $\mathbf{X}_j$ in a ball of radius r around $\mathbf{X}_i$. This number is equal to the sum $\sum_j H(r - |\mathbf{X}_i - \mathbf{X}_j|$ where H is the Heaviside function. Summing over all i and normalizing one obtains the *integral correlation function* (Grassberger and Procaccia 1983).

$$C(r) = \frac{1}{N_T^2} \sum_{ij} H(r - |\mathbf{X}_i - \mathbf{X}_j|). \qquad (11)$$

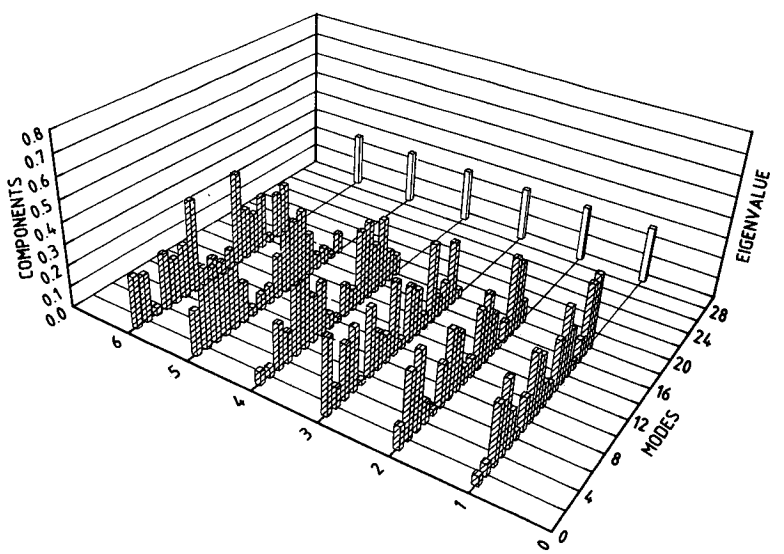

FIG. 6. As in Fig. 5, but for a pseudorandom signal.

For values of r, which are much smaller than the linear size of the attracting manifold and yet larger than scales in which sampling errors or noise may be important, one can show that C depends on r as

$$C(r) \sim r^{\nu}. \tag{12}$$

It follows that in each embedding space, ν can be estimated from the slope of the linear part of the plot of $\ln C(r)$ versus $\ln r$.

We have carried out the above algorithm using the time delay and the principal component representation, as well as using multichannel variables referring to different stations. We estimated the dimensions of manifolds and of phase spaces of the individual geopotential time series, as well as of the series obtained from their spatial average using both time lagged and multichannel variables. In phase space representation the effects of the transformation from principal to delay space is reflected by the fact that in the former the trajectory is significantly smoother than in the latter.

The calculation of the integral correlation function, Eq. (11), for both phase-space reconstructions, revealed that a lower limit of the time lag τ needed for ν to saturate to ν_s was of the order of 10 days (approximately the first zero of $\ddot{\psi}$). We increased the embedding dimensions step by step from 2 to 12. We did not increase it beyond this value in order to avoid spurious effects due to the scarcity of data points. Indeed, if the systems were embedded in higher-dimensional spaces, the interval in r for which the scaling relation of the integral correlation function holds becomes insufficient for the method to hold. Actually, this interval begins to shrink as soon as the embedding dimension becomes larger than two, mainly because the number of pairs of points available to compute the correlation function is proportional to N_T^2 while it should increase as N_T^n, where n is the embedding dimension, for the scaling interval to remain unchanged. Moreover, in excessively high-dimensional embeddings, the correlation exponent will converge for any dynamical system whatsoever, including cases of infinite-dimensional, stochastic dynamics (Caputo et al. 1986).

The distances between data points were calculated using the norm

$$\|\mathbf{X}_i - \mathbf{X}_j\| = \sum_{k=1}^{n} |X_{ik} - X_{jk}|. \tag{13}$$

Finally, for all the computations mentioned above, the correlation exponents were estimated using third order finite difference formulas involving between 10 and 20 points depending on the size of the interval in r over which the scaling relation is valid.

b. Results

We found that the two methods of phase space reconstruction gave almost identical results for each time series as well as for the computations involving the space average of all signals and a multi-channel approach. Some representative results are given in Table 1 and illustrated in Figs. 7a and 7b where $\ln C$ is plotted against $\ln r$ for the two methods and different embeddings for a single geopotential record. It is clear from the comparison of the two figures that the singular space representation reduces the effects of noise which tends to give rise to small oscillations in the plot. In Fig. 8 we represent a three-dimensional graph of the correlation exponents of the records of five different stations in spaces of increasing dimensions. Black blocks show the results using a singular phase space reconstruction whereas hatched ones are obtained using the method of delays. The upper left blocks correspond to correlation exponents of a pseudorandom signal. Interestingly, when comparing the black and hatched blocks one notes that convergence of ν toward its final value comes for about the same dimension of embedding space. Presumably this is due to the important amount of mixing occurring between EOFs corresponding to all but a few eigenvalues, thus counteracting the effects of the "optimal orthogonal set property" of the singular vectors. This corroborates the statement made in section 3, that dimensionality cannot be estimated reliably from the number of unmixed modes as suggested by Fraedrich (1986).

To have an idea of the error bar associated with our calculations we computed the dimension when the original time series is the product of two sines which as known evolves on a two-dimensional torus. The number was correctly found from both methods with an error of $\sim$0.1 or less (see also Table 1). We do not expect so small an error for our geopotential series, even though they involve the same number of samples and the same round-off error as the reference signal, mainly because the underlying dynamics seems to be much more involved. However, since the difference between the results obtained for a same attractor by the two methods never exceeds 0.3, it is likely that this gives a good idea of the error bar.

In summary, we see that the dimensionalities of all attractors analyzed are in a narrow range with a mean

TABLE 1. Generalized dimension (correlation exponent) inferred from two reconstruction methods.

Signal	Correlation exponent	
	Method of delays	Singular phase space
Lisbon	7.6	7.4
Marseille	6.8	6.7
Reykjavik	7.2	7.4
Roma	8.3	8.2
Stockholm	7.8	8.1
Space-averged	7.7	8.0
Multichannel	8.4	8.3
Two-torus	2.1	2.0

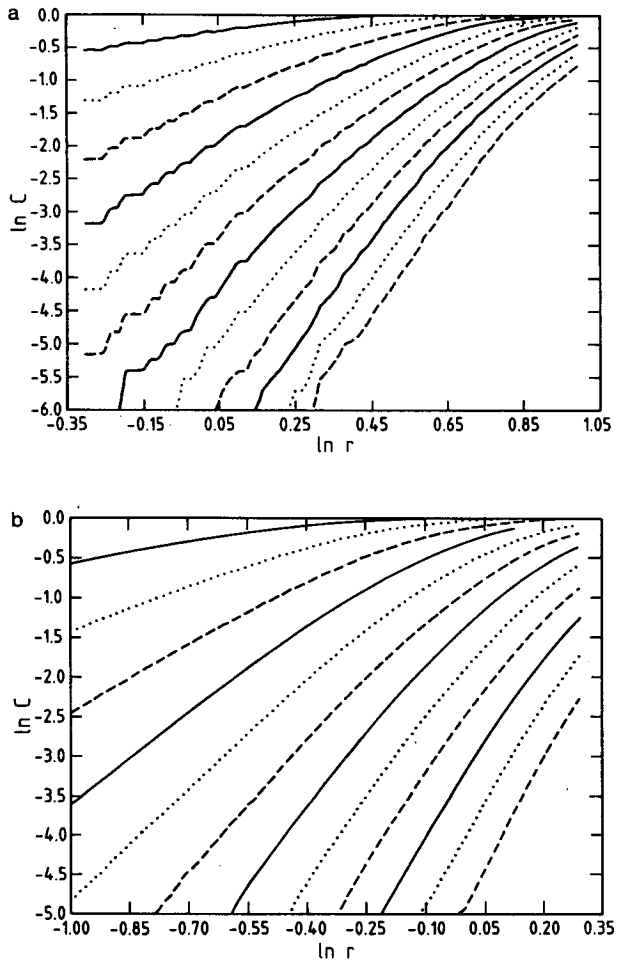

FIG. 7. Plots of ln$C$ vs ln$r$ for embedding dimensions $n = 1$ to $n = 12$ for Lisbon using method of time delays (a), and singular space (b).

value of about 7.5 and a dispersion of 10%. Consequently, it is reasonable to ascertain that the individual time series refer to a well-defined dynamical system describing the short term variability of the western European weather.

5. Lyapounov exponents: Predictability and nonuniformity

The results reported so far suggest strongly that short term weather variability over western Europe corresponds to a low-dimensional aperiodic attractor. In view of the inaccuracies in dimensionality estimates we cannot ascertain that the attractor dimension is fractal rather than integer, although the evidence for a fractal dimension is very suggestive. In this section, therefore, we examine this question from an alternative point of view, and show that the dynamics on the attractor displays sensitivity to initial conditions. Together with our previous results, this will entitle us to conclude that we are in the presence of low-dimensional chaos.

Let us formulate the problem of sensitivity to initial conditions in a quantitative manner. We imagine at time $t = 0$ a set of data included in a small n-dimensional sphere, whose center is on the attractor. The long time evolution of this sphere is subsequently monitored. We order the principal axes of this object from most rapidly to least rapidly growing and compute the mean growth rate σ_i of the ith principal axis p_i over a long period of time:

$$\sigma_i = \lim_{t\to\infty} \frac{1}{t} \int_0^t d\tau \, \frac{d}{d\tau} \ln\left(\frac{p_i(\tau)}{p_i(0)}\right)$$

$$= \lim_{t\to\infty} \frac{1}{t} \ln\left(\frac{p_i(t)}{p_i(0)}\right) \qquad (14)$$

where $p_i(0)$ is the radius of the initial sphere. The set of σ_i are referred to as *Lyapounov exponents* of the underlying dynamical system. There exist as many Lyapounov exponents as phase space dimensions (Guckenheimer and Holmes 1983). One of them is necessarily equal to zero, expressing the fact that the relative distance of initially close states on a given trajectory varies slower than exponentially. Others are negative, expressing the exponential approach of initial states to the attractor. If the dynamical system at hand is chaotic there will be at least one positive Lyapounov exponent, and the sphere will evolve to a complex ellipsoidlike form reflecting the exponential divergence of nearby initial conditions along at least one direction on the attractor. This property will be interpreted by the observer as the inability to predict the future state of the system on the basis of past knowledge of its trajectory, beyond a certain interval of time of the order of the inverse of the divergence rate. Note that in a well-behaved dissipative system the sum of all exponents must be strictly negative (Guckenheimer and Holmes 1983).

Hitherto, most analyses have provided only the largest positive Lyapounov exponent of a chaotic system. Besides, in most of the mathematical models and laboratory experiments studied so far the dimension of the chaotic attractor was between two and three, meaning that not more than one such exponent could be expected. In the problem under consideration, however, one typically deals with *hyperchaos,* manifested by attractors in the form of folded multidimensional fractal structures. In principle there is no reason to expect that unstable motion will only occur along one direction on such complex manifolds. One should therefore aim at computing as large a part of the entire *spectrum* of Lyapounov exponents as possible. To that effect we will use some algorithms developed recently in the framework of dynamical systems theory which

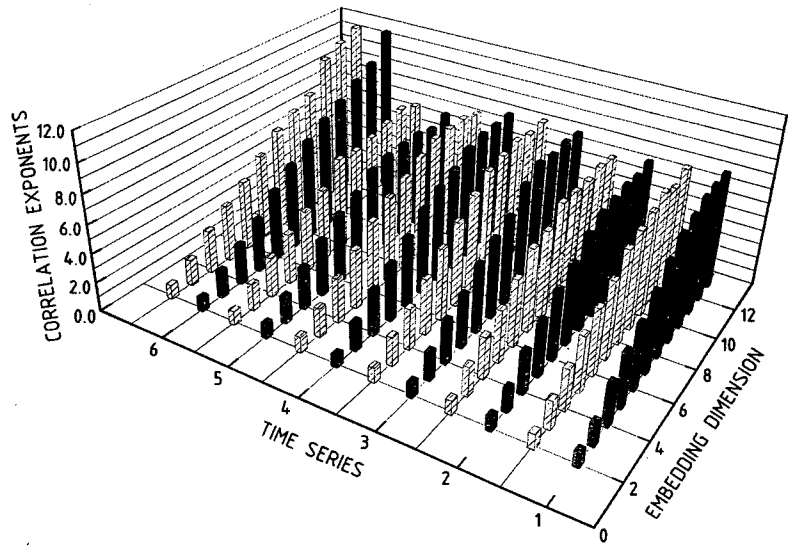

FIG. 8. Correlation exponents obtained successively by the method of time delays (hatched blocks) and by the singular space construction (black blocks) for six signals. From left to right: pseudorandom signal, 500 mb geopotential height at Marseille, Stockholm, Rome, Reykjavik and Lisbon.

allow one to compute the large amplitude exponents with reasonable accuracy (Sano and Sawada 1985; Eckmann et al. 1986).

Our analyses are mainly based on the work by Eckmann et al. (1986). The interested reader will find in the Appendix the main features of the method and some key technical details. The algorithm was first applied to one of our reference systems, the Lorenz equations, Eq. (2). We found in this case that the number of samples needed (truncated to the accuracy of data) to extract all three exponents with a reasonable error bar was of the order of 30 000! Therefore, taking into account the results reported in the previous sections, namely, that the nine stations behaved more or less as being parts of a single dynamics encompassing the whole West European weather, we reassembled the data into a single series of about 80 000 samples (see also Essex et al. 1987). We verified that the discontinuities of the signal at the connections between the different series would influence the neighborhoods of about 0.1% of the samples of the resultant concatenated time series. This would probably make the error in the estimation of the Lyapounov exponents 0.1% larger than what we would have obtained from an uninterrupted series of a single variable of the system. Using the same amount of data for the Lorenz system, we found it possible to extract the positive and zero exponents within $0.03t^{-1}$, and the negative one within 25% of its true value from a time series of the variable x. This last result is promising because the negative exponent of the Lorenz system is one order of magnitude larger than the positive one and a 25% error on its value consequently does not influence much the ratio of these two exponents which is an important qualitative property of the dynamics.

We repeated the algorithm using the concatenated series corresponding to the geopotential signal. The convergence of the algorithm to relatively sharp Lyapounov exponents was fair. Table 2 (first column) summarizes the result on the large amplitude σ_i. Several interesting conclusions can be drawn:

(i) Considering the accuracy of the method one can assert that two exponents are unmistakingly positive. Therefore, one deals here with a *hyperchaotic* attractor. The fact that the two positive σ_i are comparable in magnitude suggests that the chaotic dynamics arises from the interference of two independent mechanisms of instability of comparable importance.

(ii) There are at least three negative exponents. The absolute value of the largest among them is not significantly larger than the largest positive σ_i. This suggests that there is *no* single time scale dominating the system in the range considered.

TABLE 2. Mean and (variance)$^{1/2}$ of the most significant Lyapounov exponents deduced from the concatenated time series of the geopotential record.

Mean divergence rate σ_i (day^{-1})	(Variance)$^{1/2}$ $\Delta\sigma_i$ (day^{-1})
0.023	0.028
0.014	0.022
−0.017	0.034
−0.032	0.050
−0.079	0.101

(iii) The existence of several practically vanishing σ_i implies that the corresponding directions belong to a low-dimensional torus. It is therefore legitimate to advance the idea that the chaotic dynamics of the system arises from the fractalization of this torus.

(iv) The sum of the two largest positive exponents, equal to 0.037 day^{-1}. It gives an estimate of the metric (Kolmogorov) entropy K. Its inverse, which is about 27 days, is therefore an estimate of the mean predictability time for the geopotential signal. It is comparable, but clearly larger than the 12–17 days inferred by Fraedrich (1987) from series of about 5500 samples.

We will now discuss a way for exploring the structure of the attractor in a more detailed manner. By definition [Eq. (14)], the Lyapounov exponents are time averages over a long interval. Hence, since a typical motion on a chaotic attractor satisfies strong ergodic properties, σ_i are effectively (ensemble) averages over the entire attractor. We now introduce a finer motion on the attractor, namely the *local* rate of divergence. For this purpose we discretize time, letting η be a reasonably small step, and define

$$\beta_i(k) = \frac{1}{\eta} \ln\left(\frac{p_i(k\eta)}{p_i((k-1)\eta)}\right). \tag{15}$$

Clearly

$$\sigma_i = \lim_{N\to\infty} \frac{1}{N} \sum_{k-1}^{N} \beta_i(k). \tag{16}$$

The point is that starting from (15), one can compute numerically deviations from the averages σ_i (variances $(\Delta\sigma_i)^2$ and higher moments) or, as a matter of fact, the probability distribution for having a given local rate of divergence. Obviously the larger $\Delta\sigma_i$ (or the flatter the probability distribution), the more nonuniform the attractor will be (Nicolis 1986). The variances of the five Lyapounov exponents are given in Table 2 (second column). We see that all exponents are subjected to a very strong variability. This shows that the attractor is highly nonuniform. It is important to note that the high values of $\Delta\sigma_i$ do not compromise the sign of σ_i. Indeed, in Figs. 9a and 9b we show the histogram of the largest positive β_i, and of the most negative one. We observe in all cases a rather broad distribution, which is markedly asymmetric (toward positive and negative values, respectively). Interestingly, in these two figures the mean σ_i is rather different from the most probable value, which is close to zero. Similar trends are found for the other β_i as well.

In summary, as time varies, the system will continuously switch along the unstable directions from states of low β (large predictability) to states of high β (small predictability). We will now attempt to identify these states. To this end we follow numerically on the attractor the motion along the unstable directions corresponding to a positive rate of divergence. Since the attractor is constructed from the original time series and from a number of additional variables generated by it, this motion will necessarily run over different values of the geopotential. We will thus be able to identify the rate of divergence prevailing for different values of the geopotential.

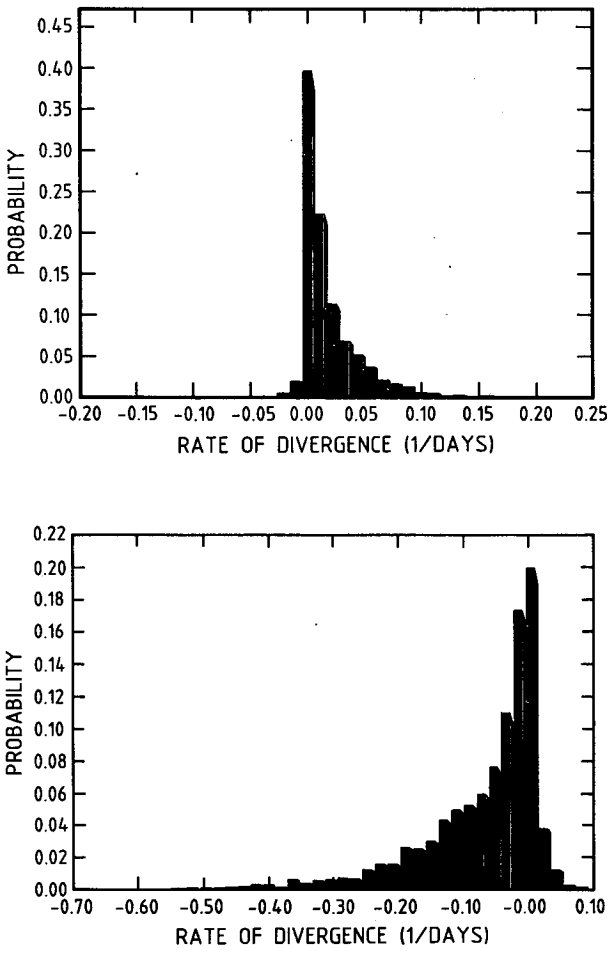

FIG. 9. Histograms of the probability distribution of the local rates of divergence β_i whose average yield (a) the largest positive Lyapounov exponent and (b) the most negative exponent.

Figure 10 summarizes the result. We consider the sum of the positive local rates, known as (local) Kolmogorov entropy (Lichtenberg and Lieberman 1983). Its inverse gives the limit of predictability of states with different geopotential values. We observe that for values corresponding to low geopotential heights the predictability is of the order of 30 days. It decreases to about 2 weeks for high geopotential values. One verifies that the mean value of these two extremes is close to the inverse of the metric entropy estimated earlier in this section.

One rather obvious idea is to relate these results with the fact that winter predictions are generally more sat-

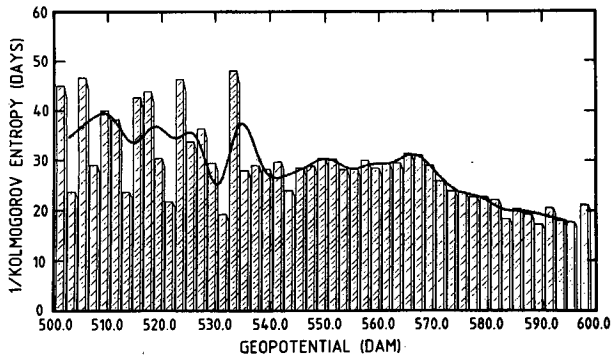

FIG. 10. Limit of predictability time expressed by the inverse Kolmogorov entropy as a function of the 500 mb geopotential height. Heavy line shows the best fit.

isfactory than summer ones. A less obvious and somewhat speculative conjecture is to associate a cyclonic weather pattern over western Europe to the Atlantic blocking (for instance, see Benzi et al. 1986). The high persistence of the latter appears therefore as the consequence of the high predictability of the low geopotential part of the attractor.

Throughout this section we have related the predictability of the atmosphere to the existence of an inherently nonlinear dynamics described by a chaotic attractor and displaying sensitivity to initial conditions. A comment on the connection between this point of view and the current use of the concept of predictability in atmospheric sciences is therefore in order.

Ordinarily, the difficulty to carry out long-term predictions of the dynamics of the atmosphere is traced back to two major elements (Lorenz 1984, 1987):

(i) Operationally, in defining the state of the atmosphere a number of errors are involved. For instance, due to the finite resolution of a measurement or of a numerical experiment, small-scale "subgrid" processes are discarded.

(ii) The principal atmospheric and climatic variables undergo complex dynamics, as a result of which small errors of the kind mentioned above are rapidly amplified. Present estimates from models of weather prediction are carried out by extrapolating to small errors the amplification times actually computed. They give error growth (doubling or *e*-folding) times of a few days. It is this time that is usually identified as the predictability time. Significantly, the growth rate seems to depend very little on the detailed nature of the error, provided that the amplitude of the latter is small enough (Lorenz 1984).

This view of atmospheric predictability is entirely compatible with the one advocated in the present paper. Indeed, whatever their detailed nature might be, subgrid processes will be perceived by the large-scale processes as a "forcing" perturbing their evolution continuously. Assuming that the forcing amplitude is small, it is then clear that the response of the large-scale processes will depend on the nature of their own dynamics, i.e., of the dynamics one is trying to predict. If the dynamics is stable the forcing will be damped: even though errors of all sorts will be arising continuously, there will be no error growth. But if, on the contrary, the dynamics is unstable the forcing will be amplified and the slightest error will grow. In short, "error growth" is above all a manifestation of a system's intrinsic instability rather than of the initial error itself, the latter acting merely as a trigger. This is also what happens in deterministic chaos: to probe the sensitivity to initial conditions one has to deviate from some basic trajectory through some initial error; but the fact that this error will be amplified and, equally importantly perhaps, the rate of its amplification, depend entirely on the dynamics.

We close this section with some remarks on the quantitative estimation of the predictability time. We have just mentioned that the current estimates of error-growth times of a few days from numerical weather prediction models involve extrapolations to the range of small errors. How are these estimates related to the predictability time of a few weeks deduced in the present paper?

Theoretically, a Lyapounov exponent from which predictability time is deduced, is an average of local rates of divergence over the attractor (or parts thereof). By definition, a local rate is a rate characterizing the response of the system in the limit of a vanishingly small deviation from a reference trajectory—a vanishingly small error. In practice, owing to the finiteness of sampling times this limit is never attained. In the problem under consideration, where the sampling time is one day, this obviously limits the analysis to errors beyond a certain size. Our results must therefore be understood in the following sense: the response of the atmosphere to errors or to disturbances in this (finite) size range, is characterized by a predictability (error growth) time of 2 to 4 weeks, depending on whether one considers the range of high or low geopotential values. Should one be able to extrapolate this estimate to small errors, a value close to Lorenz's result of a few days could conceivably come out. Such an extrapolation cannot be carried out with the type of data at our disposal.

In our view there is an additional, and perhaps subtler, aspect of this problem. Predictability is not an absolute concept but depends on the type of dynamics considered. As an example, predictability times at the level of molecular dynamics (which is known to be chaotic) are by orders of magnitude smaller than predictability times descriptive of, say, a turbulent flow. In this respect it does not make much sense to extrapolate turbulence data, whose coarseness reflects the hydrodynamic level of description, to characteristic

lengths in the molecular range and join in this way predictability estimates of molecular trajectories. We believe that a somewhat similar situation arises in the present problem. In other words, even though the daily sampled 500 mb geopotential values are inevitably affected by smaller scale processes whose predictability times might be substantially smaller, they are likely to be governed by an autonomous dynamics. This dynamics displays deterministic chaos, and is characterized by a predictability time of a few weeks. As a corollary, we suggest that there is considerable room for improving predictions of the daily 500 mb geopotential values, beyond the range of a few days.

6. Discussion

We have produced strong evidence that weather variability over western Europe, as reflected by the 500 mb geopotential values, can be accounted for by a single dynamical system of a few degrees of freedom possessing a low-dimensional attractor. We have estimated some average properties of the attractor such as its dimension and the dominant Lyapounov exponents. Furthermore, we explored its local structure and found a relation between the rate of divergence on it and the corresponding heights of geopotential.

The very possibility to describe the global dynamics by a single attractor implies the existence of long-range spatial correlations in the atmosphere, of the order of several hundreds of kilometers. The mean predictability time of three to four weeks that we found suggests that there is considerable room for improving weather predictions for phenomena belonging to this time scale. Of more interest is, perhaps, the result that predictability is actually variable and may depend on the state of the atmosphere (Lorenz 1965). This conclusion seems to be supported by meteorological experience as discussed, for instance, by Gilchrist (1986). It should be of practical value in helping to choose the adequate level of description and the degree of detail to be included in the model, when tackling a given problem.

It would be interesting to analyze from a similar point of view variability over other extended regions of the globe, as well as over time scales shorter than the one day sampling interval considered in the present work. We also believe that a dynamical systems analysis of the output of general circulation models would shed some light on the kind of variability described by these models. It should also clarify the connection between what is to be regarded as a purely statistical element or as an element reducible to some well-defined deterministic dynamics.

From a more fundamental point of view, it is our belief that the existence of intrinsically imposed limits of predictability, whatever the quality of a model might be, should have a lasting effect on the very way to model or even monitor our natural environment.

Acknowledgments. We are most grateful to J. F. Royer of the Centre National des Recherches Météorologiques, Toulouse for providing us with the data. We thank R. Benzi and M. Ghil for interesting discussions and M. Salazar for his help in the preparation of the manuscript. C. Keppenne is Research Assistant with the FNRS (Belgium). This work is supported, in part, by the European Economic Community under Contract ST2J-0079-1-B(EDB).

APPENDIX

Numerical Computation of Lyapounov Exponents

The basic steps of the algorithm used for the computation of the Lyapounov exponents may be summarized as follows (Eckmann et al. 1986; Sano and Sawada 1985):

(i) One first embeds the dataset in a d_E-dimensional space and constructs therein by the time-delay method [cf. Eqs. (7) and (8)] an orbit representing the time evolution of the system. In this space one determines the neighbors of all $\mathbf{X}_i$, i.e., the set S_i of data points $\{\mathbf{X}_j\}$ within a prescribed distance ρ from $\mathbf{X}_i$. Note that ρ must be sufficiently large for the results to be statistically significant and yet small enough to ensure the validity of the subsequent analysis [see step (ii)], based on successive linearizations of the full dynamics.

(ii) Since the Lyapounov exponents describe the mean rate of amplification of a small initial deviation from a reference trajectory [cf. Eq. (14)] we seek to construct a linear operator describing the time evolution of such deviations. Specifically, we inquire whether there exists a matrix $\mathbf{T}_i$ relating some initial displacement $\mathbf{X}_j - \mathbf{X}_i$ to its value one unit of time later, $\mathbf{X}_{j+1} - \mathbf{X}_{i+1}$

$$\mathbf{X}_{j+1} - \mathbf{X}_{i+1} = T_i(\mathbf{X}_j - \mathbf{X}_i). \tag{A1}$$

In principle the rank of this matrix, d_M need not be equal to d_E, the latter being sometimes chosen to have a rather high value. Assuming that there is an integer $m \geqslant 1$ such that

$$d_E - 1 = (d_M - 1)m \tag{A2}$$

one may then associate to the d_E-dimensional vector $\mathbf{X}_i = (X_i, X_{i+1}, \cdots, X_{i+d_E-1})$ a d_M-dimensional vector $\mathbf{Y}_i$ defined as

$$\mathbf{Y}_i = (X_i, X_{i+m}, \cdots, X_{i+(d_M-1)m}). \tag{A3}$$

Equation (A1) is thus replaced by

$$\mathbf{Y}_{j+1} - \mathbf{Y}_j = \mathbf{T}_i(\mathbf{Y}_j - \mathbf{Y}_i)$$

or equivalently:

$$\mathbf{X}_{j+m} - \mathbf{X}_{i+m} = \mathbf{T}_i(\mathbf{X}_j - \mathbf{X}_i). \tag{A4}$$

Projecting both sides of Eq. (A4) successively on the coordinate vectors of the delay space allows one to fix the $d_m - 1$ first rows of T_i by equating the coefficients of identical components of the distance vectors appearing on both sides. For the last line the above identification does not work and one has to fix the elements by a least-squares fit, requiring the difference between left- and right-hand sides of (A4) to be minimum. This yields:

$$\mathbf{T}_i = \begin{Bmatrix} 0 & 1 & 0 & & 0 \\ 0 & 0 & 1 & & 0 \\ & & & \vdots & \\ 0 & 0 & 0 & & 1 \\ a_1 & a_2 & a_3 & & a_{d_M} \end{Bmatrix} \quad \text{(A5)}$$

with

$$\sum_{j \in S_i} \Big\{ \sum_{k=0}^{d_M - 1} a_{k+1}(X_{j+km} - X_{i+km}) - (X_{j+d_M m} - X_{i+d_M m}) \Big\}^2 = \min. \quad \text{(A6)}$$

(iii) Finally, by taking the logarithmic average of the eigenvalues of $\mathbf{T}_i$ over a large number of $\mathbf{T}_i$ one obtains the average exponential rates of divergence of $\mathbf{X}_j - \mathbf{X}_i$ in phase space, which are nothing but the Lyapounov exponents for which we are looking.

REFERENCES

Abraham, N. B., A. M. Albano, B. Das, G. De Guzman, S. Yong, R. S. Gioggia, G. P. Puccioni and J. R. Tredicce, 1986: Calculating the dimension of attractors from small data sets. *Phys. Lett.*, **114A,** 217–221.

Atmanspacher, H., H. Scheingraber and W. Voges, 1988: Global scaling properties of a chaotic attractor reconstructed from experimental data. *Phys. Rev.* **37A,** 1314–1322.

Balescu, R., 1975: *Equilibrium and Nonequilibrium Statistical Mechanics.* Wiley.

Benzi, R., B. Saltzman and A. Wiin-Nielsen, Eds. 1986: Large scale anomalies and blocking. *Advances in Geophysics,* Vol. 29, Academic Press.

Brock, W., and G. Chamberlain, 1984: Spectral analysis cannot tell a macroeconometrician, whether his time series came from a stochastic economy or a deterministic economy. SSRI W.P. n° 8419, 11 pp. [Available from Department of Economics, University of WI, 1180 Observatory Drive, Madison, WI 53706.]

Broomhead, D. S., and G. P. King, 1986: Extracting qualitative dynamics from experimental data. *Physica,* **20D,** 217–236.

Caputo, J. G., B. Malmaison and P. Atten, 1986: Determination of attractor dimension and entropy for various flows: an experimentalist's viewpoint. *Dimensions and Entropies in Chaotic Systems,* G. Mayer-Kress, Ed., Springer.

Eckmann, J. P., S. Ollifson Kamphorst, D. Ruelle and S. Ciliberto, 1986: Lyapounov exponents from time series. *Phys. Rev.*, **34A,** 4971–4979.

Essex, C., T. Lookman and M. A. H. Nerenberg, 1987: The climate attractor over short timescales. *Nature,* **326,** 64–66.

Fraedrich, K., 1986: Estimating the dimensions of weather and climate attractors. *J. Atmos. Sci.*, **43,** 419–432.

——, 1987: Estimating weather and climate predictability on attractors. *J. Atmos. Sci.*, **44,** 722–728.

Ghil, M., 1987: Dynamics statistics and predictability of planetary flow regimes. *Irreversible Phenomena and Dynamical Systems Analysis in Geoscience,* C. Nicolis and G. Nicolis, Eds., Reidel, 241–283.

——, and S. Childress, 1987: *Topics in Geophysical Fluid Dynamics: Atmospheric Dynamics Dynamo Theory and Climate Dynamics.* Springer-Verlag, 479 pp.

Gilchrist, A., 1986: Long-range forecasting. *Quart. J. Roy. Meteor. Soc.*, **112,** 567–592.

Grassberger, P., 1986: Do climatic attractors exist? *Nature,* **323,** 609–612.

——, and I. Procaccia, 1983: Measuring the strangeness of strange attractors. *Physica,* **9D,** 189–208.

Guckenheimer, J., and P. Holmes, 1983: *Nonlinear Oscillations, Dynamical Systems and Bifurcations of Vector Fields.* Springer-Verlag, 453 pp.

Hasselmann, K., 1976: Stochastic climate models. Part 1: Theory. *Tellus,* **28,** 473–485.

Hense, A., 1987: On the possible existence of a strange attractor for the southern oscillation. *Beitr. Phys. Atmos.*, **60,** 34–47.

Lichtenberg, O., and M. Lieberman, 1983: *Regular and Stochastic Motion.* Springer.

Lorenz, E. N., 1963: Deterministic nonperiodic flow. *J. Atmos. Sci.*, **20,** 130–141.

——, 1965: A study of the predictability of a 28-variable atmospheric model. *Tellus,* **17,** 321–333.

——, 1984: Some aspects of atmospheric predictability. *Problems and Prospects in Long and Medium Range Weather Forecasting,* D. M. Barridge and E. Källén, Eds., Springer, 1–20.

——, 1987: Deterministic and stochastic aspects of atmospheric dynamics. *Irreversible Phenomena and Dynamical Systems Analysis in Geosciences,* C. Nicolis and G. Nicolis, Eds., Reidel, 159–179.

Mayer-Kress, G., Ed., 1986: *Dimensions and Entropies in Chaotic Systems.* Springer-Verlag, 256 pp.

Nicolis, C., and G. Nicolis, 1984: Is there a climatic attractor? *Nature,* **311,** 529–532.

——, and ——, 1985: Reconstruction of the dynamics of the climate system from time-series data. *Proc. Natl. Acad. Sci. USA,* **83,** 536–540.

——, and ——, 1987: Evidence for climatic attractors. *Nature,* **326,** 523–524.

Nicolis, J. S., 1986: Chaotic dynamics applied to information processing. *Rep. Progr. Phys.*, **49,** 1109–1196.

North, G. R., T. L. Bell, R. F. Calahan and F. J. Moeng, 1982: Sampling errors in the estimation of empirical orthogonal functions. *Mon. Wea. Rev.*, **110,** 699–706.

Rössler, O., 1979: Continuous chaos—Four prototype equations. *Ann. N.Y. Acad. Sci.*, **316,** 376–392.

Sano, M., and Y. Sawada, 1985: Measurement of the Lyapounov spectrum from a chaotic time series. *Phys. Rev. Lett.*, **53,** 1082–1085.

Takens, F., 1981: Detecting strange attractors in turbulence. *Dynamical Systems and Turbulence,* Springer-Verlag, 366–381.

Tsonis, A. A., and J. B. Elsner, 1988: The weather attractor over very short time scales. *Nature,* **333,** 545–547.

Wax, N., 1954: Selected Topics in Noise and Stochastic Processes. Dover, 337 pp.